

Analyst

Accepted Manuscript



This is an *Accepted Manuscript*, which has been through the Royal Society of Chemistry peer review process and has been accepted for publication.

Accepted Manuscripts are published online shortly after acceptance, before technical editing, formatting and proof reading. Using this free service, authors can make their results available to the community, in citable form, before we publish the edited article. We will replace this *Accepted Manuscript* with the edited and formatted *Advance Article* as soon as it is available.

You can find more information about *Accepted Manuscripts* in the [Information for Authors](#).

Please note that technical editing may introduce minor changes to the text and/or graphics, which may alter content. The journal's standard [Terms & Conditions](#) and the [Ethical guidelines](#) still apply. In no event shall the Royal Society of Chemistry be held responsible for any errors or omissions in this *Accepted Manuscript* or any consequences arising from the use of any information it contains.

1
2
3
4
5
6
7 A multi-scale approach of the mechanisms underlying exopolysaccharides auto
8
9 organization in the *Proteus mirabilis* extracellular matrix.
10
11

12
13 *Élodie Lahaye*,^{†‡} *Yun Qin*,^{‡†} *Frédéric Jamme*,^{#\$‡} *Thierry Aubry*,^{‡#} and *Olivier Sire*^{*,†‡}
14
15

16
17 Laboratoire d'Ingénierie des Matériaux de Bretagne, Université Européenne de Bretagne,
18
19 Campus de Tohannic, BP573, 56017 Vannes CEDEX, France, INRA - Département CEPIA, Rue
20
21 de la Géraudière, BP 71627, F-44316, Nantes CEDEX 3, France, Synchrotron SOLEIL, l'Orme
22
23 des merisiers Saint-Aubin BP48, 91192 Gif-sur-Yvette CEDEX, France, Laboratoire
24
25 d'Ingénierie des Matériaux de Bretagne, Université Européenne de Bretagne, UBO, UFR
26
27 Sciences et Techniques, 6, avenue Victor Le Gorgeu CS93837, 29238 Brest Cedex 3, France.
28
29
30

31
32 KEYWORDS Swarming, exopolysaccharides, auto organization, viscoelasticity, infrared
33
34 spectroscopy, synchrotron radiation
35
36

37
38 For decades, the origin of the concentric ring pattern of bacterial swarming colonies has puzzled
39
40 microbiologists. It was hypothesized that a periodic water activity variation originates a phase
41
42 transition within the extracellular matrix water H bond network, which switches on and off the
43
44 exopolysaccharides auto-organization. Both rheological and infrared spectroscopy measurements
45
46 respectively performed at a molecular scale and on a currently migrating colony, have allowed to
47
48 give a physical insight into the mechanisms which underlie the switch between swarming and
49
50 consolidation phases. Thanks to *in situ* and real time infrared microspectroscopy, and thanks to
51
52 the brilliance of the infrared beam at SOLEIL synchrotron, here we demonstrate that *Proteus*
53
54 *mirabilis* swarming is triggered by a periodic variation of water activity at the colony's edge. A
55
56
57
58
59
60

1
2
3 dynamic behavior emerges from the global properties of the multicellular entity which relies on
4
5 the ability of the bacterial cells to tune exoproducts synthesis in order to undergo sharp
6
7 transitions at a given water activity threshold.
8
9

10 11 12 13 14 Introduction

15
16
17 Bacterial colonies are excellent candidates for studying fundamental problems of self-
18
19 organization and pattern formation in complex biological systems. This is the reason why
20
21 development biologists have paid attention to multicellularity¹ since such complex systems
22
23 necessarily imply a high degree of signal integration leading to space and time correlations
24
25 linking billions of individual cells. Hence, the interest of such studies significantly overpasses
26
27 that of bacterial colonies and biofilms. In the case of *Proteus mirabilis*, it has been proposed that
28
29 the periodicity of the swarming phenomenon²⁻⁵ was linked to density-dependent thresholds in
30
31 controlling the transitions between distinct phases³. Such correlations, often observed in bacterial
32
33 multicellular entities, usually rely on chemical triggers, which mediate the quorum sensing (QS)
34
35 cell-to-cell exchanges⁶. More precisely, QS allows every cell to sense the population extent and,
36
37 beyond a given density threshold, to activate the genes responsible for differentiation or
38
39 virulence expression. Regarding this point, the *P. mirabilis* swarming constitutes a unique
40
41 complex biological oscillator. The population expands through periodic and synchronous
42
43 swarming phases which alternate with consolidation phases. If one excepts the very early stages
44
45 of the colony formation, no chemical trigger like furanones or homoserine lactones are produced
46
47 to warrant this unique synchronicity⁴. If the *flhDC* operon has been identified as the main genetic
48
49 determinant for the vegetative to swarmer cell differentiation process⁷, genetics failed to reveal
50
51 which factor was responsible for the sudden operon's switch at a given moment. Consequently,
52
53
54
55
56
57
58
59
60

1
2
3 chemical triggers were actively, but in vain, looked for⁶ since they are good candidates to convey
4 information between cells, allowing thereby to locally promoting population cohesion⁴. This
5 direction being a dead end, we turned to investigate the global properties of the colony and paid
6 attention to the biochemical and functional properties of the extra cellular matrix (ECM) that
7 constitutes the bacterial cells continuum^{8,9}. The *P. mirabilis* ECM biochemical analysis revealed
8 a binary mixture of exopolisaccharides (EPS), a phenoglycolipid (PGL) and glycine betaine
9 (GB), a well-known bacterial osmoprotectant. The presence of GB and of a PGL strongly
10 suggested that the bacterial colony is submitted to a permanent osmotic stress, which in turn
11 indicates that water content may constitute a constraint.
12
13
14
15
16
17
18
19
20
21
22
23
24

25 Here we present a multi-scale approach of the mechanisms which underlie the periodic and
26 synchronous swarming of *P. mirabilis*. Earlier studies^{8,9} have suggested that ECM, due to its
27 viscoelastic properties and its ability to form spherulites would behave as a semi-crystalline
28 continuum. The present paper aims at bringing evidence that such properties are deeply involved
29 in a periodic variation of water activity (a_w), which in turn is responsible for the morphotype's
30 switch between swarming and consolidation phases (see Fig. 10 in ⁸). To demonstrate that this
31 switch between consolidation and swarming phases is controlled by an EPS phase transition in
32 relation to ECM water activity, experiments were performed to characterize more thoroughly the
33 EPS viscoelastic properties and to monitor, *in situ* and in real-time, the EPS auto-organization
34 along with the water H bonds network.
35
36
37
38
39
40
41
42
43
44
45
46
47
48
49
50
51
52
53

54 Experimental Section

55
56
57
58
59
60

1
2
3 Strain, Media and Culture Conditions. The *P. mirabilis* wild-type strain WT19 corresponds to
4 the clinical isolate U64507. WT19 was grown in LB medium at 37 °C. To obtain homogeneous
5 populations of swarmer bacteria, 200 µL of an overnight liquid culture was spread onto a LB
6 agar (1.5%) plate, and the latter was incubated for 4 h at 37 °C. For studying the periodic
7 swarming, a 3 µL inoculum was deposited at the center of a Petri dish and was allowed to grow
8 for up to 8 hours on the same agar solid medium.
9
10
11
12
13
14
15
16
17
18
19
20
21

22 Experimental techniques.
23
24

25 Exopolysaccharides Extraction and Purification. EPS extraction and purification from actively
26 swarming colonies have essentially been performed as described in ⁸. As previously mentioned,
27 the EPS fraction from a swarming colony is essentially characterized by two compounds with
28 different molecular weights, one with a low molecular weight of 1 kDa and the other with a
29 much higher molecular of 400 kDa, in a 20:1 ratio.
30
31
32
33
34
35
36
37

38 Polarized Microscopy. Purified EPS solutions at different concentrations (wt. %) have been
39 prepared and were allowed to age between a sealed slide and coverslip. Observations are
40 performed by using a BX-60 polarizing microscope and a quarter wave plate.
41
42
43
44
45

46 Rheology. All rheological measurements were carried out in oscillatory simple shear with a
47 controlled strain rheometer (TA Instruments), equipped with a cone and plate geometry (cone
48 angle: 2°, diameter: 5cm). The sample temperature was set at 20°C using a thermostatic bath. For
49 each sample tested, strain sweep viscoelastic tests were first performed at a fixed 1 Hz frequency
50 in order to determine the extent of the linear regime; then, frequency sweep experiments were
51
52
53
54
55
56
57
58
59
60

1
2
3 carried out at a fixed strain in the linear regime in order to determine the linear viscoelastic
4
5 moduli, that is the storage modulus G' and the loss modulus G'' , of the samples. G' characterizes
6
7 the elastic energy stored in the sample structure, and G'' the viscous dissipation within the
8
9 sample. Purified EPS solutions at six different concentrations, 4.8 wt.%, 9 wt.%, 13 wt.%, 16.7
10
11 wt.%, 23 wt.%, and 28 wt.%, have been characterized.
12
13
14

15
16 Infrared Spectroscopy. The Mid Infrared (MIR) spectroscopy has for long been used to probe
17
18 macromolecule structures and conformations since and, hence, is well suited to monitor EPS
19
20 auto-organization¹²⁻¹⁴ which shows up in the 1200-900 cm^{-1} frequency domain^{12,13}. Water is
21
22 also a strong absorbent in the MIR domain due to the O-H stretching (localized around 3400
23
24 cm^{-1}) and the H-O-H bending (localized at 1640 cm^{-1}) vibrations. Unfortunately, due to
25
26 significant spectral overlap, essentially with proteins, the colony water content cannot be
27
28 straightforwardly derived from absorbencies in these domains. This drawback may be bypassed
29
30 by monitoring instead the water librational band located at around 615 cm^{-1} ¹³⁻¹⁵. This band is
31
32 rarely used since most of the optics and detectors of infrared spectrophotometers are non-
33
34 transparent and not sensitive enough, respectively, to yield a signal with sufficient SNR to be
35
36 interpreted. Another technical difficulty is that bacterial colonies exhibit high absorbency and
37
38 diffusivity in the infrared domain which prevent from collecting a high quality specular reflected
39
40 signal, the unique acquisition mode to get spectral information without any physical contact
41
42 between the optics and a currently migrating colony. As a consequence, a very brilliant IR source
43
44 is required, which is only available at a synchrotron radiation facility. Hence, to simultaneously
45
46 monitor the EPS auto-organization phenomena and a_w variations during a complete swarming
47
48 phase, we used synchrotron infrared microspectroscopy (Continuum and NicPlan, Nicolet
49
50 microscopes) allowing a satisfying (15 μm) 2D spatial resolution, and two types of IR detectors:
51
52
53
54
55
56
57
58
59
60

1
2
3 a MCT detector (Continuum) to firstly assess *in situ* the occurrence of EPS auto-organization,
4
5 and, secondly, a Si:B bolometer (NicPlan) which allows to record IR spectra in the 2000-400
6
7 cm^{-1} wavenumber range which encompasses both EPS and water librational absorption bands.
8
9
10 Spectra are the average of 126 scans and are collected at a 4 cm^{-1} spectral resolution during a
11
12 complete swarming cycle (consolidation-swarming-consolidation). It must be noted that no
13
14 significant baseline drifts were observed nor artefacts generally arising from Mie scattering.
15
16 Hence no Kramers-Kronig correction was applied to the collected spectra and intensities are
17
18 expressed as $\log(1/R)$. This allows assessing that the observed spectral changes are not due to
19
20 standing wave effects as described by Filik¹⁶.
21
22
23
24
25
26
27
28

29 Results and discussion

30
31
32 Semi-crystallinity of the EPS purified fraction. In the present study, ECM is assumed to play a
33
34 major role in the switch between consolidation and swarming phases of *P. mirabilis* colonies.
35
36 This hypothesis relies on the semi-crystalline properties of this continuum. Previous SEM
37
38 experiments have shown that spherulite-like objects were observed in colonies⁹, whereas
39
40 spherulites and needle-like crystalline objects were observed in purified ECM fractions⁸. Since
41
42 a_w variations within the colony are expected to drive reversible EPS auto-organization, we made
43
44 attempts to study the behavior of EPS solutions at various concentrations to highlight the relation
45
46 between a_w and the formation of semi-crystalline objects. Hence, observation of EPS solutions at
47
48 different concentrations (wt.%) were performed by using polarizing optical microscopy.
49
50
51
52
53
54
55
56
57
58
59
60

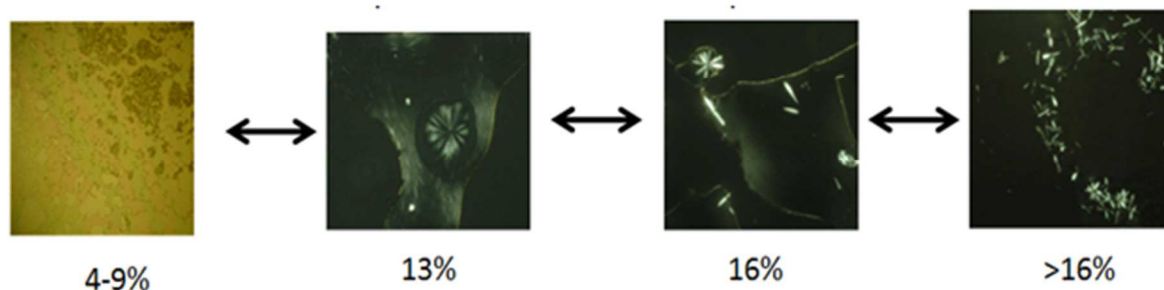
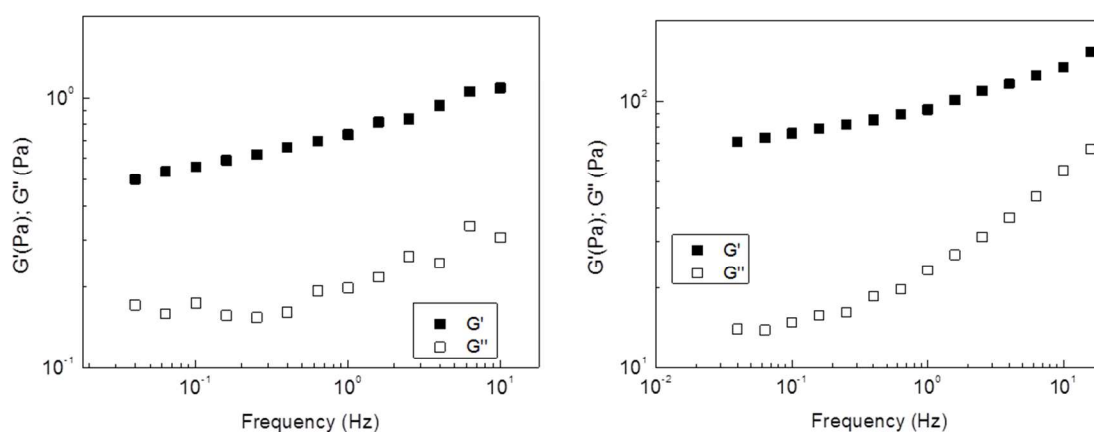


Figure 1. Crystalline objects observed by polarized microscopy at different purified EPS weight fractions. The frame widths are 700 μm .

Figure 1 displays different objects observed at weight concentrations ranging from 5 up to 28%. At low weight concentrations ($<10\%$), the micrographs do not show any particular objects. At a concentration of about 13 wt.%, spherulite-like objects appear, with a strongly birefringent signature due to local order; they exhibit diameters ranging from 100 up to 200 μm . If the water activity is further decreased, radially ordered crystalline needle-like objects are observed, which look very much like those observed by SEM in a swarming colony (see Fig. 6 in ⁹). These needle-like objects exhibit an average length l of about 100 μm and an average diameter D of about 17 μm , leading to an average aspect ratio l/D of about 6 (about 50 needles were characterized). These observations clearly show that, in a *P. mirabilis* colony, such semi-crystalline objects are derived from EPS auto-organization and are independent on any effect due to, or mediated by, the bacterial cells, since these objects are observed in EPS purified solutions. Above 16 wt.%, a new structure, governed by auto-organization phenomena, appears as suggested by the observation of crystalline needle-like objects organized in a branched network, which is expected to give an additional contribution to the ECM rigidity. It was hence necessary to further characterize the mechanical properties of the ECM, in the concentration range on both sides of the concentration corresponding to the above-described structural change.

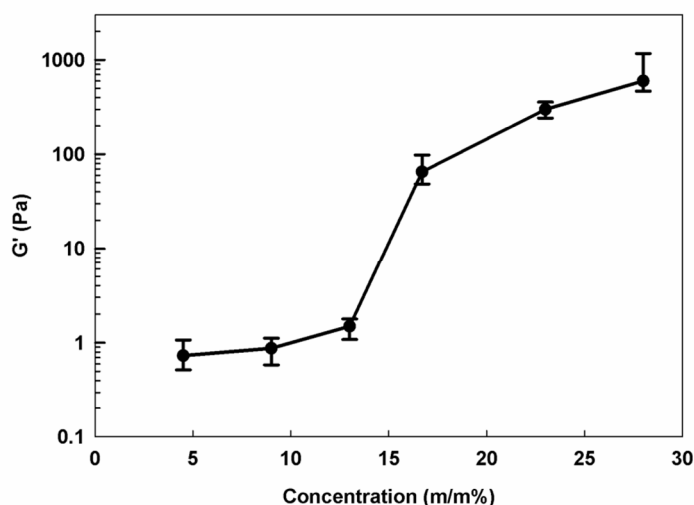
1
2
3 Mechanical properties of the EPS purified fraction. For all samples tested, the limit of the
4 linear viscoelastic regime, where G' and G'' are independent of strain amplitude, lies between
5
6 0.1% and 1%. This result shows that a low strain is able to induce a non-linear viscoelastic
7
8 behavior, suggesting that the structure of the EPS solutions, over the whole range of
9
10 concentrations investigated, is rather fragile.
11
12
13
14
15
16
17
18
19

20 Figure 2 shows the storage modulus G' and the loss modulus G'' as a function of frequency, at
21 a strain chosen in the linear response regime, for a 4.8 wt% (Fig.2A) and 16.7 wt% (Fig.2B) EPS
22 solution, respectively. At all EPS concentrations investigated in this work, the viscoelastic
23 behavior of EPS solutions has the same features: both viscoelastic moduli have low values and
24 are weakly dependent on frequency, at least in the frequency range investigated, and $G' \gg G''$.
25
26 These results mean that all EPS solutions investigated in this work behave like soft viscoelastic
27 solids, which suggests that their structure is that of a weak gel¹⁷, most likely due to the presence
28 of numerous H bonds which connect EPS molecules, forming a fragile three-dimensional
29 polymeric network, as discussed in a previous paper⁸.
30
31
32
33
34
35
36
37
38
39
40
41
42
43
44
45
46
47
48
49
50
51
52
53
54
55
56
57
58
59
60



1
2
3 Figure 2 Storage modulus G' and loss modulus G'' as a function of frequency, at a fixed strain
4 amplitude of 0.5%, for a 4.8 wt% (Left) and 16.7 wt% (Right) EPS solution.
5
6
7
8

9 The main difference between the low and high concentrated EPS solutions is the level of the
10 moduli: the storage modulus of a 16.7 wt% EPS solution is about 2 decades higher than that of a
11 4.8 wt% EPS solution. In order to study the EPS concentration dependence of the storage G' at a
12 fixed frequency, we plotted Figure 3.
13
14
15
16
17
18
19



20
21
22
23
24
25
26
27
28
29
30
31
32
33
34
35
36
37
38
39 Figure 3: Storage modulus G' as a function of EPS concentration, at a frequency of 1 Hz.

40
41
42 Figure 3 clearly shows that there are two concentration regimes: at EPS concentrations below
43 about 13 wt%, G' has low values and exhibits a weak concentration dependence, whereas at EPS
44 concentrations higher than 15 wt%, G' has much higher values and exhibits a much stronger
45 concentration dependence. One may refer to Fig. 1 for the corresponding supramolecular
46 organization present at each concentration.
47
48
49
50
51
52
53
54

55 The existence of a concentration threshold at about 13 wt%, characterized by a drastic G'
56 increase, has to be linked with the concentration induced modification of the state of
57
58
59
60

1
2
3 organization of the EPS macromolecules presented above. Indeed the presence of anisometric
4
5 needle-like crystalline entities (the so-called spicules, see Fig. 1) in EPS solutions at
6
7 concentrations higher than 10 wt% could be responsible for the drastic enhancement of elastic
8
9 properties.
10

11
12
13
14 Knowing the characteristic dimensions of crystalline needles, and the percolation volume
15
16 fraction of spheres, $\Phi_{ps} \sim 30\%$ ¹⁸, the percolation volume fraction, Φ_p , of these objects can be
17
18 inferred from the assumption that the volume occupied by cylinders is equivalent to that of
19
20 spheres with a radius equal to half the average length of the cylinders. Indeed, if the needles are
21
22 considered as cylinders, with diameter D and length L , then :

$$\frac{\Phi_p}{\Phi_{ps}} = \frac{3}{2} \left(\frac{D}{L} \right)^2$$

23
24
25
26
27
28
29
30
31
32 Knowing the average aspect ratio of the microcrystalline spicules $L/D \sim 6$, then $\Phi_p \sim 1.3\%$;
33
34 thus only about 1 vol% spicules are needed to form a percolation network. We suggest that the
35
36 EPS concentration threshold at about 13 wt% corresponds to the percolation threshold of the
37
38 microcrystalline spicules, and that, above this concentration threshold, the significantly enhanced
39
40 elastic response of EPS solutions is due to the superposition of the EPS transient polymeric
41
42 network and the spicule percolation network.
43
44
45
46

47
48 Rheological experiments performed on EPS solutions have revealed a marked elastic
49
50 behaviour with a sharp phase transition driven by water activity. Such a behaviour is the
51
52 signature of EPS auto-organization, which in turn depends on the physico-chemical modulation
53
54 of polysaccharides H bond networks. At low a_w , a percolation network is formed which is
55
56 expected to drastically hinder swarm cell motility. Since an alteration of the external medium
57
58
59
60

1
2
3 mechanical properties drives the initial cell differentiation subsequent to the transfer of the strain
4
5 from a liquid culture to an agar Petri dish¹⁰, we have hypothesized that the periodicity and
6
7 synchronicity of the swarming could be ruled by a_w variations at the edge of the colony. Both
8
9 experimental observations and theoretical considerations^{9, 11} converge to suggest that, due to the
10
11 colony spreading on the agar as a thin (15 μm) film during a swarming phase, the resulting
12
13 increased S/V ratio would increase the net water transfer from the agar to the colony. The
14
15 resulting increased a_w within the biofilm should consequently induce a disorganization of the
16
17 percolation network which is responsible for the high storage modulus of the EPS solutions. It
18
19 was then necessary to look for concomitant variations of both EPS supramolecular organization
20
21 and water H bonds network. These attempts have been performed through infrared
22
23
24
25
26
27
28
29
30
31
32
33
34
35
36
37
38
39
40
41
42
43
44
45
46
47
48
49
50
51
52
53
54
55
56
57
58
59
60

microspectroscopy on a currently swarming colony.

Real time study of EPS auto-organization. We firstly attempt to assess *in situ* the occurrence of
EPS auto-organization by monitoring, in a non-invasive way, the EPS MIR spectral domain
through an entire swarming cycle, *i.e.* between two consecutive consolidation phases. Every two
minutes, a spectrum was collected at the colony's moving edge, which allows spatially mapping
the spectral information. Figure 4 shows the resulting MIR spectra.

.....

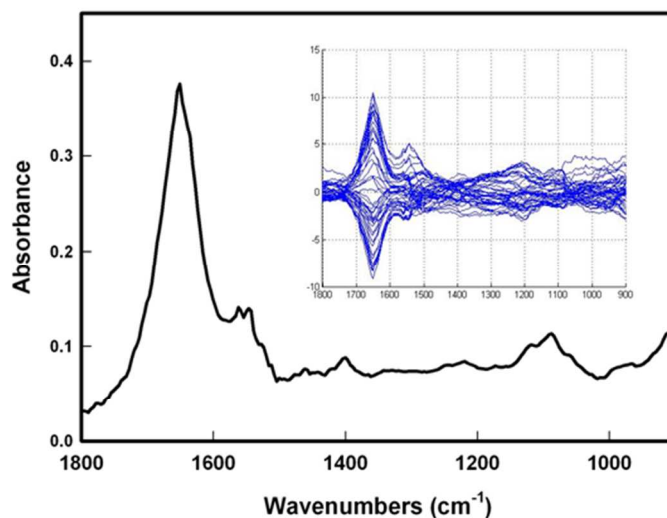


Figure 4. Mean MIR spectrum (1800-900 cm^{-1}) and difference spectra (inset) of a currently swarming colony. The figure displays the average ($n=50$) spectrum in the 1800-900 cm^{-1} frequency domain and the inset shows the dynamic spectra (from which the mean spectrum has been subtracted). Proteins Amide I and II bands show up at 1650 cm^{-1} (with a strong overlap of the water bending mode) and 1540-1580 cm^{-1} , respectively whereas EPS show up in the 1200-900 cm^{-1} frequency domain.

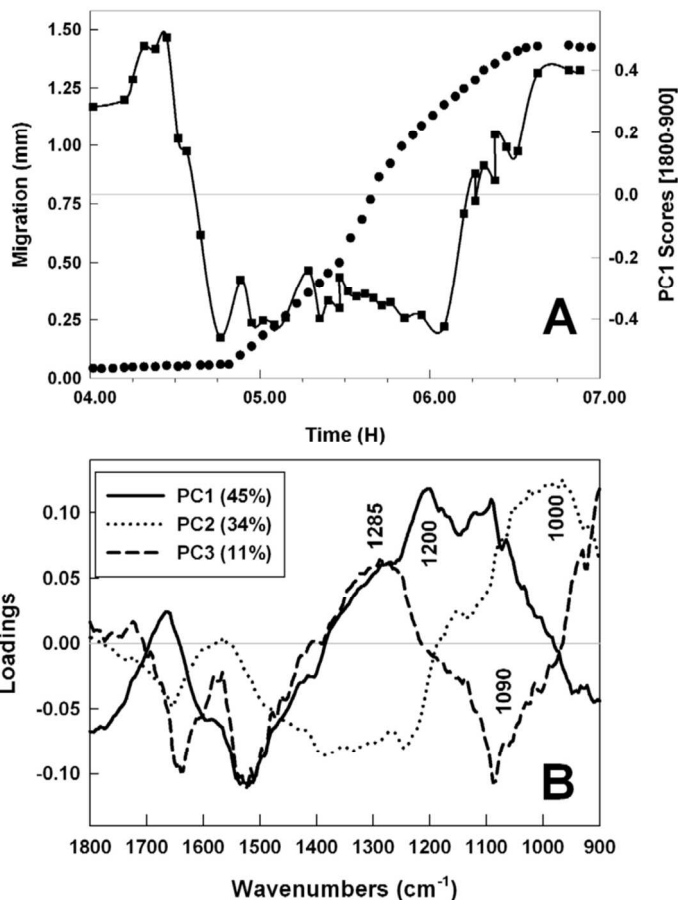


Figure 5. PCA of MIR spectra ($1800\text{-}900\text{ cm}^{-1}$) collected during a swarming phase. A: The migration (dots) scale is zeroed at the beginning of the experiment and corresponds to an initial colony radius of approximately 3 mm, The PC1 score is also plotted (solid line); B: Three first principal components.

The data set was analysed by Principal Component Analysis (PCA), and the first principal component featuring 45% of the total variability was plotted as a function of the colony expansion (Fig. 5A). The resulting data show that most of the spectral variations can be safely assigned to EPS since the three first PCs, reflecting up to 90% of the total variability, are dominated by spectral features which correspond to the EPS absorption domain (Fig. 5B). It is

1
2
3 noteworthy that the PC1 scores (Fig. 5A) undergo a reversible sharp transition just before the
4 colony's edge switches between swarming and consolidation. Hence, it can be assessed that the
5
6
7
8
9
10
11
12
13
14
15
16
17
18
19
20
21
22
23
24
25
26
27
28
29
30
31
32
33
34
35
36
37
38
39
40
41
42
43
44
45
46
47
48
49
50
51
52
53
54
55
56
57
58
59
60

noteworthy that the PC1 scores (Fig. 5A) undergo a reversible sharp transition just before the colony's edge switches between swarming and consolidation. Hence, it can be assessed that the EPS auto-organization which has been observed on purified EPS solutions^{8,19}, also occurs *in situ* at the transition between consolidation and swarming phases.

In order to determine whether or not EPS auto-organization is linked to a_w variations within the colony, IR spectra were collected on a lower spectral window encompassing both the EPS and water librational mode frequency domains. This was made possible by the use of a Si:B bolometer, which is much more sensitive in this low frequency domain than the MCT detector.

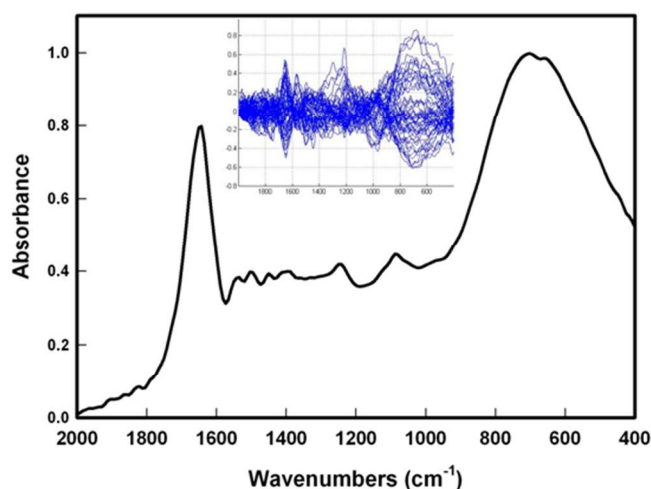


Figure 6. Mean MIR spectrum (2000-400 cm⁻¹) and difference spectra (inset) of a currently swarming colony. The figure displays the average ($n=57$) spectrum while the inset displays the corresponding dynamic spectra. The broad band located at 615 cm⁻¹ features the water librational mode; the dynamic spectra emphasize the variations of absorbance in this domain.

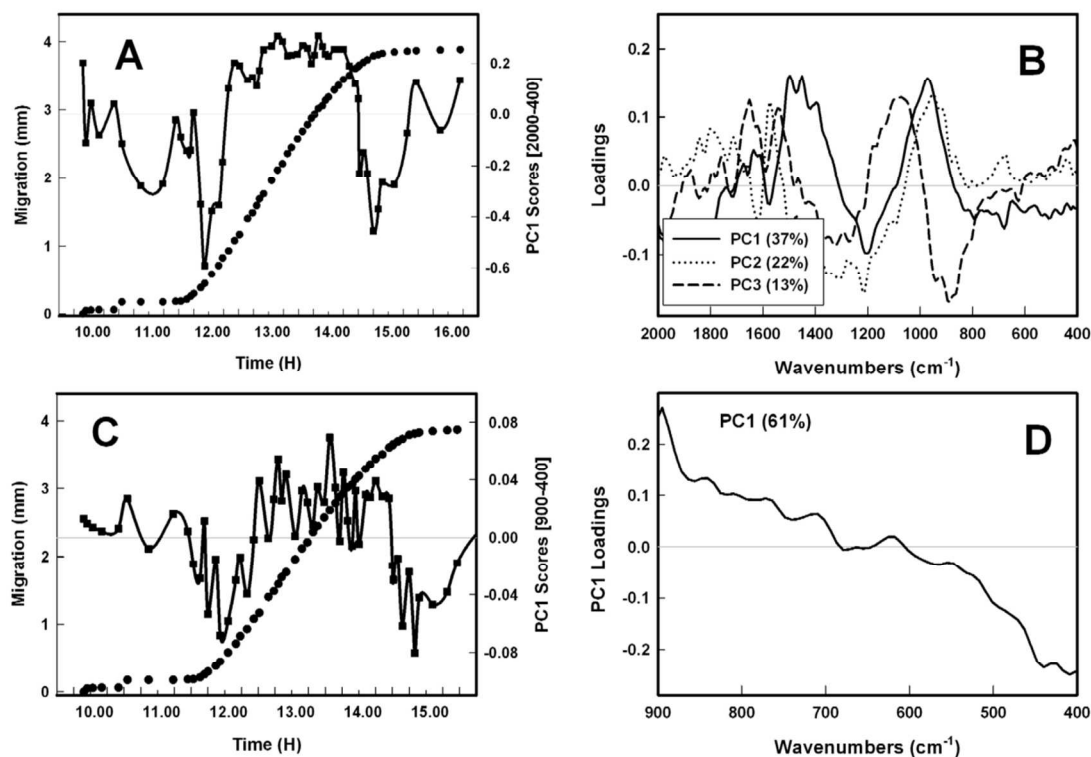


Figure 7. PCA of MIR spectra ($2000\text{--}400\text{ cm}^{-1}$) collected during a swarming phase. Spectra were collected with the NicPlan microscope. A first PCA (A, B) was performed by using the whole spectral domain ($2000\text{--}400\text{ cm}^{-1}$). A second PCA (C, D) was performed on the sole water absorption domain ($900\text{--}400\text{ cm}^{-1}$). A and C: migration, dots; PC1 scores, solid line.

Fig. 6 shows the mean spectrum and the amplitude variations of the data set collected, as previously, during a full swarming cycle. Besides variations in the EPS spectral domain, significant variations are also observed in the spectral range that corresponds to the water librational mode, *i.e.* from 900 to 400 cm^{-1} . To correlate EPS auto-organization observable between 2000 and 900 cm^{-1} with a_w variations observable from the 615 cm^{-1} water librational band, a first PCA (Fig. 7A, B) was performed by using the whole spectral domain ($2000\text{--}400\text{ cm}^{-1}$) which again reflects major changes in the EPS absorption domain as shown in Fig. 7B.

1
2
3 To emphasize spectral variations of the water librational mode, a second PCA (Fig. 7C, D) was
4 performed on the sole water absorption domain (900-400 cm^{-1}) which demonstrates that during
5 active swarming (here from 11h30 to 14h30), IR spectra exhibit positive PC1 loadings which
6 correspond to low absorbencies at the low frequency band tail, and hence low a_w . Indeed, the
7 corresponding PC1 loadings (Fig. 7D) show that during swarming, the water band loses intensity
8 over its lower energy side. This spectral evolution has been reported (see Fig. 2C in ¹⁵) to reflect
9 an increased crystallinity or, in other words, a larger H bonds connectivity. The data shown are
10 from one representative experiment which has been reproduced on three distinct colonies. One
11 must note that the PC1 score variation in the 900-400 cm^{-1} domain is an order of magnitude less
12 than one observed in the 2000-400 cm^{-1} one.
13
14
15
16
17
18
19
20
21
22
23
24
25
26
27

28 To investigate the causality between the changes in EPS H bond networks and water activity, a
29 2D correlation analysis was performed²⁰. The corresponding synchronous 2D correlation map
30 (Fig. 8A) indicates that the spectral envelope between 950 and 1050 cm^{-1} decreases as the 500 to
31 800 cm^{-1} domain increases. Indeed, in a 2D synchronous map, negative cross peaks reflect bands
32 that evolve in an opposite manner during the process²⁰. Information about the time sequence of
33 these spectral variations can be derived from 2D asynchronous maps. The Fig. 8B shows a part
34 of the upper left corner of the corresponding 2D asynchronous map. The negative cross peak
35 centred at 1000 / 700 cm^{-1} allows to establish that the EPS vibrational bands are altered after the
36 water ones^{20,21}; hence, changes in the water H bond networks at the colony's edge precede any
37 EPS auto-organization.
38
39
40
41
42
43
44
45
46
47
48
49
50
51
52
53
54
55
56
57
58
59
60

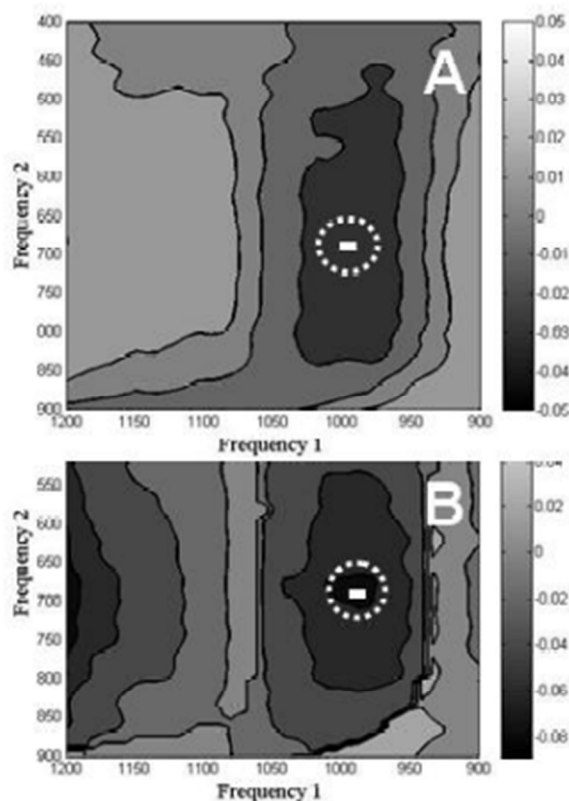


Figure 8. 2D IR synchronous (A) and asynchronous (B) maps.

Knowing that polysaccharides solutions allow forming a percolation network, the subsequent sharp increase of the elastic modulus must be linked to the periodic ability of the colony to swarm and consolidate. In this scheme, consolidation onset must be triggered by the connectivity transition, which appears in the abrupt increase of the elastic properties shown in Fig.3, which efficiently impairs swarming.

A wide infrared transparency window combined with the brilliance of the IR synchrotron beam at SOLEIL has allowed us, for the first time, to simultaneously monitor, in a non-invasive way and real time, the water H bond network and the EPS auto-organization within a currently swarming colony. Statistical data analysis (PCA and 2D correlation spectroscopy) have allowed

1
2
3 establishing that a_w periodic variations and the resulting water H-bonding alterations do
4
5 periodically occur and trigger EPS auto-organization. The progressive decrease of bulk water
6
7 molecules during a swarming phase promotes additional elastic constraints due to the onset of a
8
9 percolation network. Eventually, the inability of bacterial cells to keep swarming will trigger
10
11 dedifferentiation to enter a new consolidation phase. Hence, the extensive correlation which links
12
13 individual cells over large distances originates in a global property of the multicellular entity.
14
15
16 The periodic water gradient at the colony's edge associated to volumetric variations of the
17
18 colony which spreads from a "thick" ($> 45 \mu\text{m}$) consolidation terrace to a "thin" ($16 \mu\text{m}$)
19
20 swarming film warrants for the synchrony of swarming. This exemplifies how biological
21
22 properties and physical laws interplay: the bacterial cells synthesize a mixture of exoproducts
23
24 (EPS, PGL, GB) whose structure is tuned to undergo marked transitions as passing over a given
25
26 threshold. The *P. mirabilis* exoproducts differ whether the strain is grown in a liquid culture or
27
28 on a solid medium⁸; this further supports that the ability of bacterial populations to cope with
29
30 distinct environments tightly relies on the behaviour of such macromolecules.
31
32
33
34
35
36

37
38 In conclusion, the periodic and synchronous population behaviour is not controlled by a chemical
39
40 trigger, but rather derives from the efficiency of supramolecular assemblies to respond to an
41
42 external stimulus yielding thereby a high structural order over large dimensions which here has
43
44 been characterized as a percolation network. These results concerning the *P. mirabilis* biologic
45
46 oscillator are of broad significance since they demonstrate how the supramolecular behaviour of
47
48 macromolecules promotes complex embedded dynamic cycles which root the evolution from
49
50 unicellularity to multicellularity and, eventually, to pluricellularity : the permanent osmotic force
51
52 allows polysaccharides self-organization to promote cyclic dissipative structures.
53
54
55
56
57
58
59
60

1
2
3 ASSOCIATED CONTENT
4
5

6
7 **Supporting Information.** 2D synchronous and asynchronous full color maps are available on
8
9 the journal web site
10

11
12 AUTHOR INFORMATION
13

14
15 **Corresponding Author**
16

17 * Corresponding author. E-mail : osire@univ-ubs.fr. Phone:++ 33 297 017 148. Fax: ++ 33 297
18
19 017 071.
20

21
22 †Laboratoire d'Ingénierie des Matériaux de Bretagne, Vannes, Université Européenne de
23
24 Bretagne.
25
26

27
28 ††INRA - Département CEPIA.
29
30

31
32 §Synchrotron SOLEIL.
33
34

35 #Laboratoire d'Ingénierie des Matériaux de Bretagne, Brest, Université Européenne de Bretagne.
36
37

38
39 **Author Contributions**
40

41 The manuscript was written through contributions of all authors. All authors have given approval
42
43 to the final version of the manuscript. ‡These authors contributed equally.
44
45

46
47 **Funding Sources**
48

49 The authors gratefully acknowledge the financial support of the Region Bretagne.
50
51

52
53 ACKNOWLEDGMENT
54
55
56
57
58
59
60

1
2
3 Experiments have been performed at the synchrotron SOLEIL on the beamline/station SMIS in
4
5 the framework of proposals 20060121 and 20080395. The Authors are grateful to Dr Paul
6
7 Dumas, SMIS beamline manager, for support and discussion. The authors acknowledge the
8
9 French National Institute for Agricultural Research (INRA) and especially Pr Alain Buleon for
10
11 helpful discussions..
12
13

14 15 16 ABBREVIATIONS

17
18 a_w : water activity; ECM: extra cellular matrix; EPS: exopolysaccharides; ATR-FTIR: attenuated
19
20 total reflexion-Fourier transform infrared; GB: glycinebetaine; LB: Luria Bertani; PGL:
21
22 phenoglycolipid; SEM: Scanning Electron Microscopy; SVR: surface to volume ratio.
23
24
25
26
27

28 29 REFERENCES

- 30
31 (1) Shapiro, J. A. in *Bacteria as Multicellular Organisms*, J. A. Shapiro, M. Dworkin Eds.
32
33 (Oxford University Press, New York, 1997), pp. 14-49.
34
35
36
37 (2) Allison, C. & Hugues, C. Closely linked genetic loci required for swarm cell
38
39 differentiation and multicellular migration by *Proteus mirabilis*. *Mol. Microbiol.* 1991, 5, 1975-
40
41 1982.
42
43
44 (3) Rauprich, O., Matsushita, M., Weijer, C. J., Siegert, F., Esipov S. E. & Shapiro J. A.
45
46 Periodic phenomena in *Proteus mirabilis* swarm colony development. *J. Bacteriol.* 1996, 178,
47
48 6525-6538.
49
50
51
52 (4) Fraser G. M. & Hugues, C. Swarming motility. *Curr. Opinion Microbiol.* 1999, 2, 630-
53
54 635.
55
56
57
58
59
60

- 1
2
3 (5) Matsuyama, T., Takagi, Y., Nakagawa, Y., Itoh, H., Wakita, J. & Matsushita M.
4
5 Dynamic aspects of the structured cell population in a swarming colony of *Proteus mirabilis*. J.
6
7 Bacteriol. 2000, 182, 385-393.
8
9
10
11 (6) Costerton, J. W., Lewandowski, Z., Caldwell, D. E., Korber D. R. & Lappin-Scott. H. M.
12
13 Microbial biofilm. Annu. Rev. Microbiol. 1995, 49, 711-745.
14
15
16
17 (7) Eberl, L., Christiansen, G., Molin, S. & Givskov, M. Differentiation of *Serratia*
18
19 *liquefaciens* into swarm cells is controlled by the expression of the *flhD* master operon. J.
20
21 Bacteriol. 1996, 178, 554-559.
22
23
24
25 (8) Lahaye, E., Aubry, T., Kervarec, N., Douzenel, P. & Sire, O. Does water activity rule *P.*
26
27 *mirabilis* periodic swarming ? I. Biochemical and functional properties of the extracellular
28
29 matrix. Biomacromol. 2007, 8, 1218-1227.
30
31
32
33 (9) Lahaye, E., Aubry, T., Fleury, V. & Sire, O. Does water activity rule *P. mirabilis* periodic
34
35 swarming ? II. Viscoelasticity and water balance during swarming. Biomacromol. 2007, 8, 1228-
36
37 1235.
38
39
40
41 (10) Allison, C., Lai, H.-C., Gygi D. & Hugues C. Cell differentiation of *Proteus mirabilis* is
42
43 initiated by glutamine, a specific chemoattractant for swarming cells. Mol. Microbiol. 1993, 8,
44
45 53-60.
46
47
48
49 (11) Frenod, E. & Sire, O. An explanatory model to validate the way water activity rules
50
51 periodic terrace generation in *Proteus mirabilis* swarm. J. Math. Biol. 2009, 59, 439-466.
52
53
54
55
56
57
58
59
60

1
2
3 (12) Keirsse, J., Lahaye, E., Bouter, A., Dupont, V., Boussard-Pledel, C., Bureau, B., Adam,
4 J.-L., Monbet, V. & Sire, O. Mapping bacterial surface population physiology in real-time:
5 infrared spectroscopy of *Proteus mirabilis* swarm colonies. *Appl. Spectrosc.* 2006, 60, 584-591.
6
7

8
9
10 (13) Haxaire, K., Marechal, Y., Milas, M. & Rinaudo, M. Hydration of polysaccharide
11 hyaluronan observed by IR spectrometry. I. Preliminary experiments and band assignments.
12 *Biopolymers* 2003, 72, 10-20.
13
14
15

16 (14) Haxaire, K., Marechal, Y., Milas, M. & Rinaudo, M. Hydration of polysaccharide
17 hyaluronan observed by IR spectrometry. II. Definition and quantitative analysis of elementary
18 hydration spectra and water uptake. *Biopolymers* 2003, 72, 149-161.
19
20
21
22
23
24
25
26

27 (15) Brubach, J.-B., Mermet, A., Filabozzi, A., Gerschel, A. & Roy, P. Signatures of the
28 hydrogen bonding in the infrared bands of water. *J. Chem. Phys.* 2005, 122, 184509.
29
30
31
32

33 (16) Filik, J., Frogley, M. D., Pijanka, J., Wehbe, K., Cinque, G. Optical standing-waves
34 artifacts in reflection-absorption FTIR microscopy of biological materials. *J. Physics* 2012, 359,
35 012006.
36
37
38
39
40

41 (17) Larson R.G. In *The Structure and Rheology of Complex Fluids*; Oxford University Press:
42 New York, 1999.
43
44
45

46 (18) Consiglio, R.; Baker, D.R.; Paul, G.; Stanley, H.E. Continuum percolation thresholds for
47 mixtures of spheres of different sizes. *Physica A* 2003, 319, 49-55.
48
49
50
51
52
53
54
55
56
57
58
59
60

1
2
3 (19) Gué, M., Dupont, V., Dufour, A. & Sire, O. Bacterial swarming: a biochemical time-
4 resolved FTIR-ATR study of *Proteus mirabilis* swarm-cell differentiation. *Biochemistry* 2001, 4,
5 11938-11945.
6
7
8

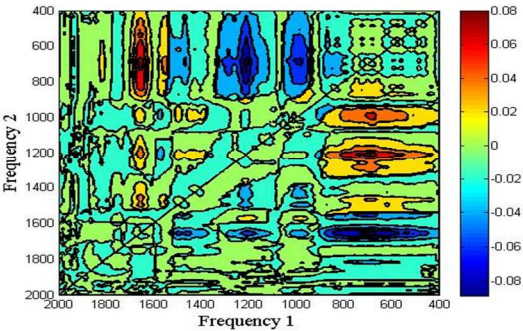
9
10
11 (20) Noda, I. Advances in two-dimensional correlation spectroscopy. *Vib. Spectrosc.* 2004,
12 36, 143-165.
13
14
15

16
17 (21) Czarnik-Matusiewicz, B., Pilorz, S., Ashton, L. & Blanch, E. W. Potential pitfalls
18 concerning visualization of the 2D results. *J. Mol. Struct.* 2006, 799, 253-258.
19
20
21

22
23 (22) Lahaye, E.; Aubry, T.; Kervarec, N.; Douzenel, P.; Sire O. Does water rule *P.mirabilis*
24 periodic swarming ? I. Biochemical and functional properties of the extra cellular matrix.
25 *Biomacromolecules* 2007, 8, 1218-1227.
26
27
28
29
30
31
32
33
34
35
36
37
38
39
40
41
42
43
44
45
46
47
48
49
50
51
52
53
54
55
56
57
58
59
60

Table of Contents graphic

For Table of Contents Use Only

	<p>A multi-scale approach of the mechanisms underlying exopolysaccharides auto-organization in the <i>Proteus mirabilis</i> extracellular matrix</p> <p>Elodie Lahaye, Yun Qin, Frederic Jamme, Thierry Aubry and Olivier Sire*</p>	
--	---	--